Amino acid sensing by the α-cell mitochondrial phosphoenolpyruvate cycle regulates intracellular Ca^{2+} levels without impacting glucagon secretion

Erli Jin[1], Hannah R. Foster[1], Evgeniy Potapenko[1], Shih Ming Huang[1], Xinhang Dong[2], Jing W. Hughes[2], and Matthew J. Merrins[1,3]

[1]Department of Medicine, Division of Endocrinology, Diabetes, and Metabolism, University of Wisconsin-Madison, Madison, WI 53705, USA

[2]Department of Cell Biology and Physiology, Washington University School of Medicine, St. Louis, MO 63110, USA

[3]William S. Middleton Memorial Veterans Hospital, Madison, WI 53705, USA

*Correspondence: mmerrins@medicine.wisc.edu (M.J.M)

Keywords: Glucagon secretion, pancreatic α-cells, amino acid metabolism, pyruvate kinase, mitochondrial phosphoenolpyruvate carboxykinase.

Abstract

Objective: Pancreatic islet α-cells are increasingly recognized as amino acid sensors for the organism, however the metabolic pathways that α-cells use to sense amino acids have not been identified. Building on our prior work in β-cells, we sought to determine whether the mitochondrial phosphoenolpyruvate (PEP) cycle is involved in α-cell amino acid sensing.

Methods: To investigate amino acid regulation of α-cells at the cellular level, we measured intracellular Ca^{2+} (GCaMP6s imaging), membrane potential (JEDI-2P imaging and patch-clamp), K_{ATP} channel activity, and glucagon secretion. Three different methods were used to probe the PEP cycle, including pyruvate kinase activators (TEPP-46), and mice with α-cell specific deletion of pyruvate kinase M1/M2 (PKM1/2-αKO) or mitochondrial PEP carboxykinase (PCK2-αKO).

Results: The mitochondrial fuels glutamine/leucine antagonized alanine/arginine-stimulated Ca^{2+} influx and glucagon secretion under hypoglycemic conditions. Both pyruvate kinase and PCK2 were required for glutamine/leucine to close K_{ATP} channels and limit amino acid-stimulated membrane depolarization. The Ca^{2+} response to amino acids was blocked by pyruvate kinase activation with TEPP-46, and enhanced by α-cell deletion of pyruvate kinase or PCK2 – all without changing glucagon secretion. Finally, using diazoxide/KCl to probe the pathways downstream of membrane depolarization, we identified an essential role of the PEP cycle in homeostatically restoring intracellular Ca^{2+} levels.

Conclusions: The α-cell mitochondrial PEP cycle senses glutamine/leucine and inhibits K_{ATP} channels similarly to β-cells, while restricting amino acid stimulated membrane depolarization and Ca^{2+} influx. However, none of the amino acids tested, including alanine/arginine, regulate glucagon secretion by modulating membrane depolarization or intracellular Ca^{2+}.

Highlights

- Our studies identify a role for the α-cell PEP cycle in sensing amino acids under hypoglycemic conditions.

- Pyruvate kinase and PCK2 are required for glutamine/leucine to close α-cell K_{ATP} channels and limit membrane depolarization and Ca^{2+} influx.
- Glutamine/leucine oppose alanine/arginine-stimulated Ca^{2+} influx and glucagon secretion.
- All of the amino acids tested regulate glucagon secretion, but none do so by modulating membrane depolarization or intracellular Ca^{2+} levels.

1. Introduction

Glucagon release from pancreatic islet α-cells is elevated under fasting and hypoglycemic conditions. Under these conditions, when inhibitory paracrine signals from neighboring islet β/δ-cells are reduced, α-cells respond strongly to non-glucose fuels including fatty acids and amino acids, which modulate Ca^{2+} and glucagon secretion [1–5]. Glucagon secretion is dependent on voltage-dependent Ca^{2+} channels (VDCC) [6–8], which trigger downstream endoplasmic reticulum Ca^{2+} release [9]. The activity of these channels is tightly regulated by membrane potential (V_m). Among the many ion channels that regulate α-cell V_m, the activity of ATP-sensitive K^+ (K_{ATP}) channels is thought to be an important determinant of α-cell V_m, Ca^{2+}, and glucagon release [10–15]. When glucose is elevated, glycolysis inhibits α-cell K_{ATP} channels and restricts Ca^{2+} entry [10,16–20]. However, the metabolic pathways that control α-cell function in response to amino acid stimulation remain unknown.

How exactly do individual amino acids impact glucagon secretion? The mechanisms are diverse. Some amino acids, like glutamate and glycine, stimulate glucagon secretion through α-cell membrane receptors [21–23]. Charged amino acids like arginine may stimulate Ca^{2+} influx by directly depolarizing V_m [24,25]. Alanine, which is uncharged, may also regulate V_m due to co-transport with Na^+ [26,27]. In contrast, the branched chain amino acids are inhibitory to glucagon release [28–30]. Leucine, for example, has been shown to suppress glucagon release by lowering cAMP, both via a direct effect on the α-cell and by stimulating inhibitory paracrine signaling via β/δ-cells [31]. Beyond secretion, glutamine is required for amino acid stimulated α-cell proliferation [32], a mechanism that links glucagon release to amino acid catabolism in the liver-α-cell axis [3,33]. Each of these findings indicate that amino acids are crucial to α-cell viability and function, but little is known about their intracellular metabolism.

In this paper, we focused on the mitochondrial fuels glutamine and leucine, and their control of α-cell V_m and Ca^{2+} by the glucagonotropic amino acids alanine and arginine. Due to the paucity of α-cell data, our working model was based on prior work in β-cells [18,34,35]. At low glucose, glutamine and leucine evoke insulin secretion by stimulating mitochondrial phosphoenolpyruvate (PEP) production by the PCK2 enzyme. Mitochondria PEP is then used by plasma-membrane associated pyruvate kinase (PK), which raises the ATP/ADP ratio to close K_{ATP} channels, depolarize V_m, and open VDCC [18,34–36]. In the PEP cycle, pyruvate generated by the PK reaction is sequentially metabolized by mitochondrial pyruvate carboxylase and PCK2, and returned to cytosol as PEP to augment flux through PK. Similar to β-cells, α-cell K_{ATP} channels are locally controlled by plasma membrane-associated enzymes including PK [18]. However, these experiments were performed using excised patch-clamp, leaving it unclear whether PK and the PEP cycle are active in α-cells and if they regulate V_m, Ca^{2+}, or glucagon secretion.

2. Results

2.1. Glutamine and leucine suppress α-cell Ca^{2+} influx stimulated by alanine and arginine

Mixed amino acids, provided at their concentrations measured in mouse portal blood (QLRA; 0.6 mM glutamine, 0.5 mM leucine, 0.2 mM arginine, 2 mM alanine) [26], stimulated biphasic glucagon secretion from mouse islets under low glucose conditions (Figure 1A). To determine how amino acids regulate α-cell Ca^{2+}, we imaged islets isolated from mice expressing GCaMP6s biosensors in α-cells (*GcgCre^{ERT}:GCaMP6s*). Although single α-cells exhibited heterogeneity in their Ca^{2+} response, the aggregate islet response to mixed amino acids was a sustained rise in Ca^{2+} (Figure 1B). Opening K_{ATP} channels with 200 μM diazoxide (Figure 1C) or blocking L-type VDCCs with 1 μM isradipine (Figure 1D) suppressed the Ca^{2+} rise stimulated by amino acids, confirming the requirement for membrane depolarization and L-type VDCCs [6,9,15].

We applied various combinations of amino acids at low glucose to identify their individual effects on α-cell Ca^{2+}. Arginine induced only a transient Ca^{2+} rise, while alanine provoked a sustained increase (Figure 1E,F). The effects of arginine and alanine were additive. On their own, the combination of glutamine and leucine only slightly reduced average Ca^{2+}, however, they impaired the intracellular Ca^{2+} response to alanine and arginine by 42% (cf. Figures 1G and 1H). In a perifusion assay, glutamine and leucine suppressed glucagon secretion stimulated by arginine and alanine (Figure 1I). Glucagon release fell in response to glutamine withdrawal, and the glucagonostatic effect of leucine was reduced (Figure 1J). Taken together, alanine and arginine stimulate Ca^{2+} influx and glucagon secretion, while the combination of glutamine and leucine has a suppressive effect. Since amino acids were applied to the entire islet in theses assays, the inhibitory effects of paracrine signaling cannot be completely ignored (*e.g.*, glutamine/leucine stimulate insulin release, Supplemental Figure 1). We therefore sought additional approaches to isolate the effects of amino acids on α-cell metabolism.

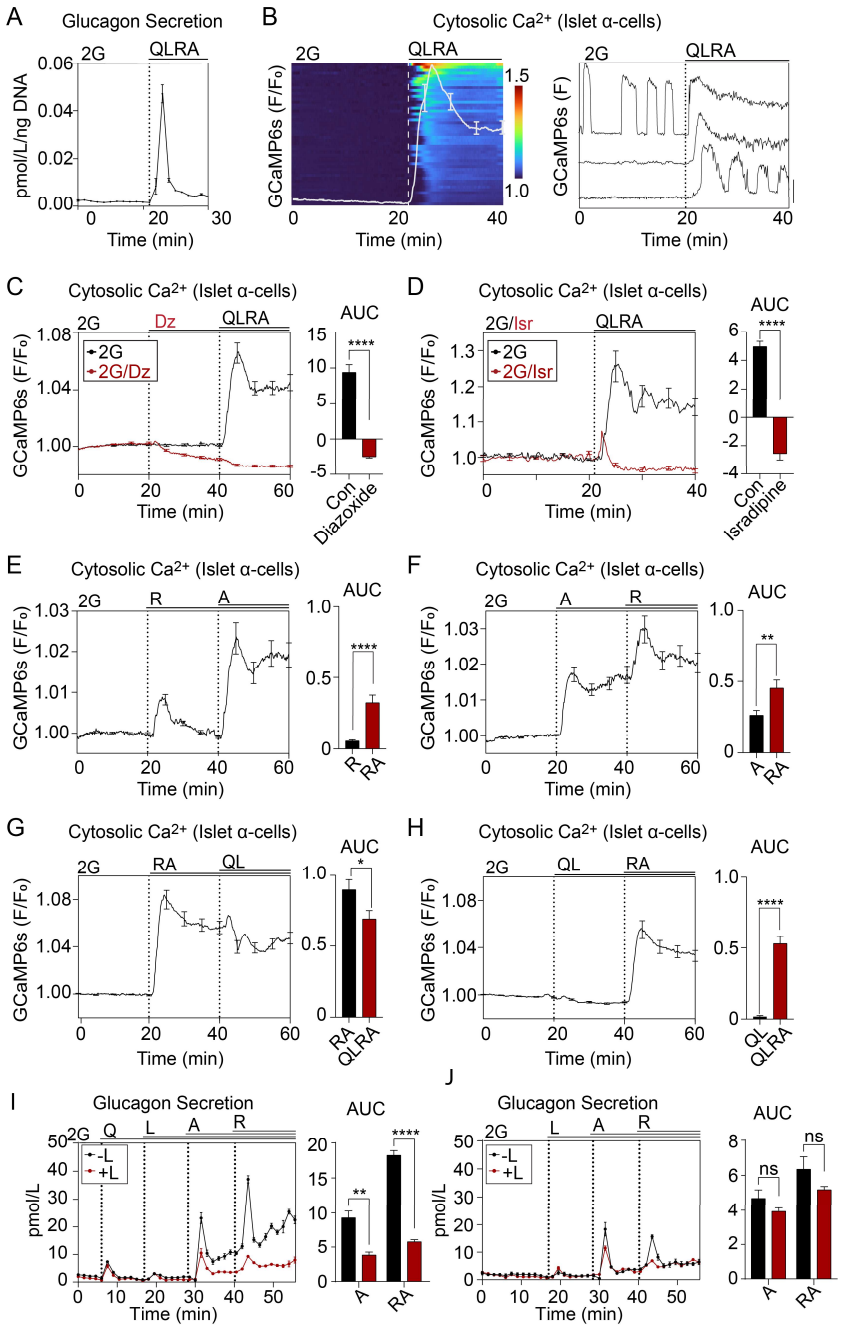

Figure 1. Glutamine/leucine suppress α-cell Ca^{2+} influx stimulated by alanine/arginine. (A) Perifusion assay was used to measure glucagon secretion from mouse islets in the presence of 2 mM glucose (2G) and amino acids (QLRA, in mM: 0.6 mM glutamine, 0.5 mM leucine, 0.2 mM arginine, 2 mM and alanine). (B) Heatmap (left) and example traces (right) of Ca^{2+} responses in intact mouse islets expressing GCaMP6s biosensors. Average Ca^{2+} is shown in the white trace (left panel). (C-D) Amino acid stimulated Ca^{2+} influx is blocked by 200μM diazoxide (K_{ATP} channel opener) (C) and 10 μM isradipine (L-type VDCC blocker) (D). (E-J) α-cell Ca^{2+} (E-H) and glucagon secretion (I-J) stimulated by QLRA alone or in combination. Imaging data (B-H) represent averaged normalized GCaMP6s intensity from n = 40-56 islets from 3 mice imaged per protocol. Perifusion data (A, I, and J) represent the average of n = 3 chambers from n = 3 mice per

condition with 80–100 mouse islets per chamber. Data are shown as mean ± SEM with AUC for each condition compared with control by Student's *t* test. **P* < 0.05, ***P* < 0.01, *****P* < 0.0001.

2.2. Mice lacking α-cell PKM1/2 or PCK2 respond normally to changing glucose levels

To test the function of the α-cell PEP cycle, we generated mice with α-cell specific knockout of PKM1/2 or PCK2 by crossing *GcgCre^{ERT}:GCaMP6s* mice with *Pkm$^{f/f}$* mice (PKM1/2-αKO, *GcgCre^{ERT}:GCaMP6s:Pkm$^{f/f}$)* or *Pck2$^{f/f}$* mice (PCK2-αKO, *GcgCre^{ERT}:GCaMP6s:Pck2$^{f/f}$*). All studies were performed with littermate *GcgCre^{ERT}:GCaMP6s* controls. α-Cell specific knockdown of PKM1/2 and PCK2 was evident by immunostaining of isolated islets (Figure 2A,B), however high background fluorescence made absolute quantification difficult. After pooling FACS-sorted GCaMP6s^{+} α-cells from 6 mice per genotype, we confirmed by Western blot that PKM1 and PKM2 were virtually absent in α-cells from PKM1/2-αKO islets (Figure 2C). Although PCK2 was undetectable by Western blot, we confirmed the loss of *Pck2* mRNA using QPCR of FACS-sorted α-cells; *Pck2* mRNA was reduced by 88% in PCK2-αKO α-cells relative to controls.

To investigate glycemic control in the PKM1/2-αKO and PCK2-αKO mice, we performed meal tolerance tests (MTT) by gavage of protein shake after a 5 hour fast. No differences in blood glucose clearance were observed in the PCK2-αKO mice relative to controls (Figure 2D). A small improvement in glucose tolerance was observed in the PCK2-αKO mice relative to controls, however this effect appears to be driven by elevated glucose in the control mice at a single timepoint (Figure 2E). To test the function of PKM1/2-αKO and PCK2-αKO mice under low glucose conditions, fasted mice were subjected to an insulin tolerance test. No difference in fasting glucagon was observed in either strain, and insulin lowered blood glucose and stimulated glucagon secretion to a similar extent in PKM1/2-αKO and PCK2-αKO mice as controls (Figure 2F,G). Thus, both strains of knockout mice responded normally to raising or lowering blood glucose.

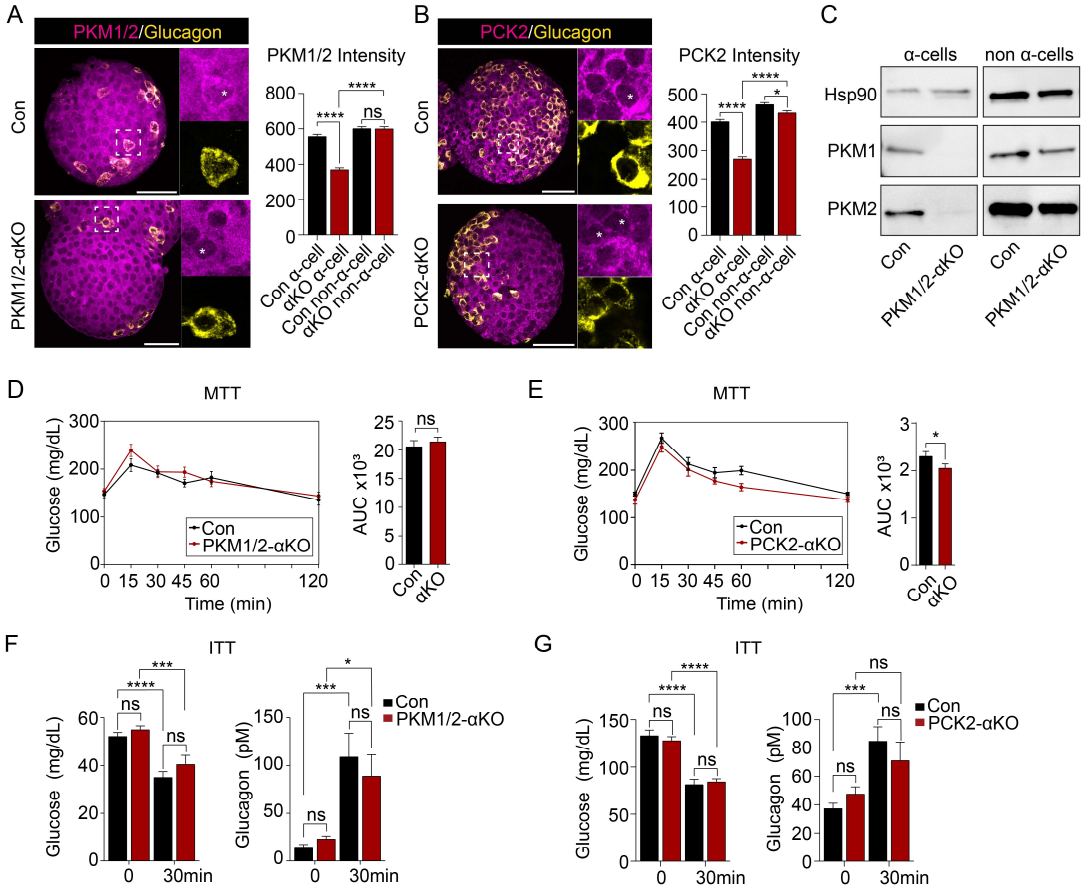

Figure 2. Mice lacking α-cell PKM1/2 or PCK2 respond normally to changing glucose levels. (A-B) Representative images of stained islets showing targeted deletion of PCK2 in Glucagon$^+$ α-cells. Insets highlight α-cells (asterisks) with intact (control) or reduced (PCK2-αKO) enzyme expression. Scale bar, 50 µm. Quantification represents n = 100 cells from 10 islets per genotype. (C) Western blot showing PKM1/2 knockdown in FACS sorted α-cells (GCaMP6s$^+$) and non-α-cells (GCaMP6s$^-$) from PKM1/2-αKO and controls (pooled samples from 6 mice per group). (D-E) Meal tolerance test (MTT) with PKM1/2 and PCK2 α-KO. n = 10 mice per group. (F-G) Plasma glucose and glucagon levels in PKM1/2-αKO, PCK2α-KO, and littermate controls in response to an insulin tolerance test (ITT). Data are shown as mean ± SEM with AUC for each condition compared with control by Student's t test (C-D) or one-way ANOVA (B, E-F). *$P < 0.05$, ***$P < 0.001$, ****P < 0.0001, ns, not significant

2.3. The α-cell PEP cycle closes K_{ATP} channels and restricts V_m depolarization in response to amino acid stimulation

Previous studies in β-cells show that, at low glucose, glutamine and leucine stimulate insulin secretion by fueling the mitochondrial PEP cycle to close K_{ATP} channels, depolarize V_m, and open VDCCs [35]. Given that α-cell K_{ATP} channels are also regulated by PK [18], we tested whether the PEP cycle impacts electrical activity similarly in α-cells. K_{ATP} channel activity was directly measured by patch-clamp using the fluorescent GCaMP6s reporter to positively identify α-cells. K_{ATP} channel activity was increased by glutamine and reduced by leucine in the control group, effects that were blunted or blocked by α-cell deletion of PKM1/2 and PCK2 (Figures 3A

and 3B). Notably, leucine retained some ability to close K_{ATP} channels in the PKM1/2-αKO, while failing to close K_{ATP} channels in the PCK2-αKO cells. These data suggest that the remaining α-cell PKL isoform can partially compensate for the loss of PKM1/PKM2, while cutting off the mitochondrial PEP supply for all three PK isoforms (i.e., by deleting PCK2) is more severe.

We next tested how PEP cycle affects α-cell V_m using perforated patch-clamp recordings of surface α-cells in the intact islet. α-Cells were identified by their characteristic I-V curves (Supplemental Figure 2). The application of mixed amino acids (QLRA) depolarized α-cell V_m by 4.7 mV on average in control islets (Figure 3C). Relative to controls, the amino acid-stimulated increase in ΔV_m trended upward in PKM1/2-αKO α-cells, but only reached significance in the PCK2-αKO (Figure 3C,D). Given the high degree of α-cell variability, and the low throughput inherent to the patch-clamp approach, we performed orthogonal measurements using JEDI-2P voltage sensors [37] to record ΔV_m from hundreds of α-cells. In these assays, we isolated islets from PKM1/2-αKO and PCK2-αKO mice without GCaMP6s. Voltage-sensitive JEDI-2P biosensors [37] were expressed in α-cells using Cre-dependent adenovirus. Islets from PKM1/2-αKO and PCK2-αKO mice were measured simultaneously with their controls using barcoding with near-IR dyes. Confirming the patch-clamp studies, the α-cell ΔV_m response to amino acids was augmented by deletion of PCK2, while α-cell deletion of PKM1/2 had no significant effect (Figure 3E,F).

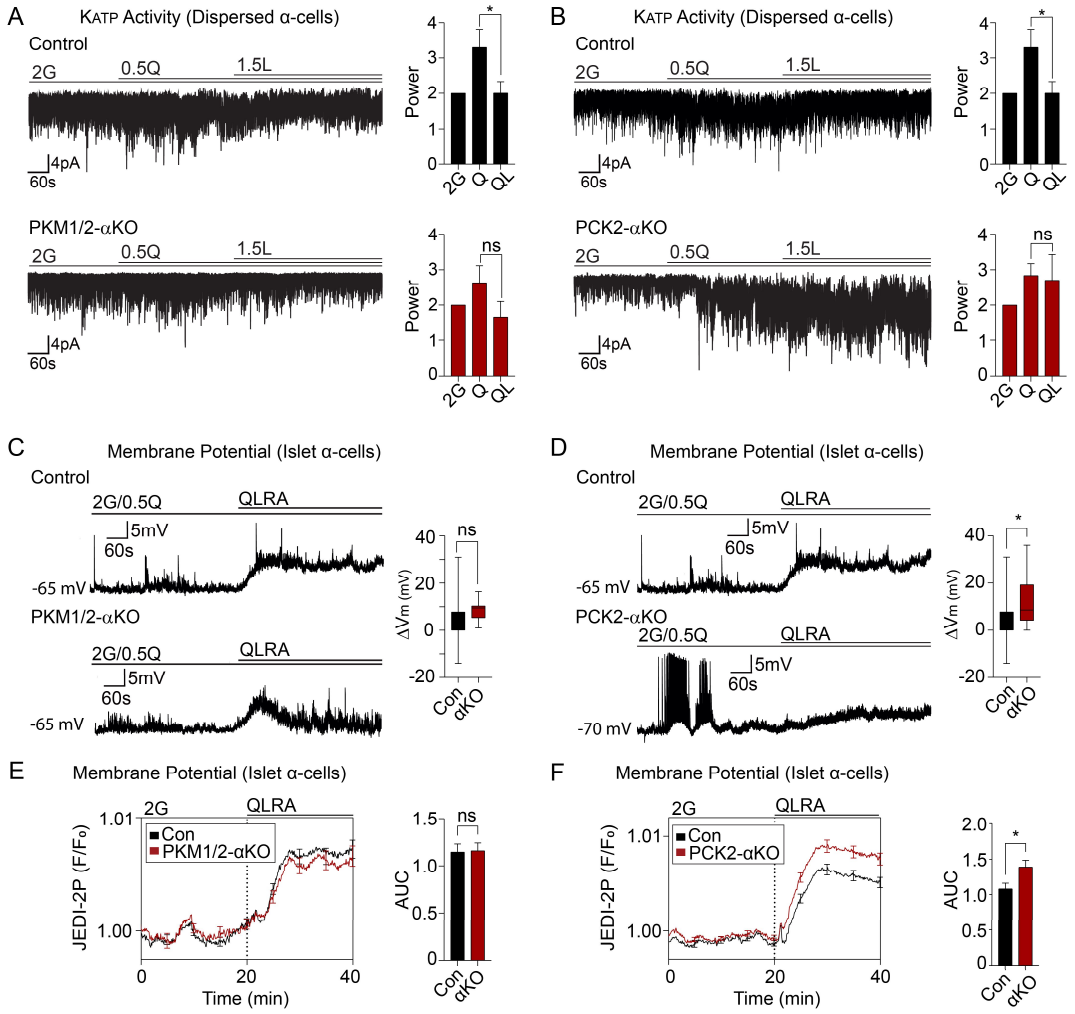

Figure 3. The α-cell PEP cycle closes K_{ATP} channels and restricts α-cell membrane potential in response to amino acid stimulation. (A-B) Example traces and power analysis of K_{ATP} channel activity in response to 0.5 mM glutamine (0.5Q) and 1.5 mM leucine (1.5L) in dispersed α-cells from PKM1/2-αKO (A) and PCK2-αKO (B) and controls. (C- D) Example traces and membrane potential (ΔV_m) measured by patch-clamp in response 2 mM glucose and amino acids (QLRA; 0.6 mM glutamine, 0.5 mM leucine, 0.2 mM arginine, 2 mM and alanine) in intact islets from PKM1/2-αKO (C) and PCK2-αKO mice (D) as indicated. Data represent 12-18 cells from 3 mice per group. (E-F) Average normalized membrane potential (ΔV_m) measured by JEDI-2P voltage sensors in response to 2 mM glucose and QLRA in islets from PKM1/2-αKO (E) and PCK2-αKO mice (F) as indicated. Data represent 64-92 islets from 3 mice imaged per protocol. Data are shown as mean ± SEM for each condition compared with control by either by one way ANOVA (A, B) or Student's *t* test (*C–F*). Controls were averaged in A-B and C-D. *$P < 0.05$, ns, not significant.

2.4. The PEP cycle suppresses α-cell Ca^{2+} in response to amino acid stimulation without impacting glucagon release

Our electrophysiological analyses of K_{ATP} channels and V_m suggested a mechanism by which PKM1/2 and PCK2 might regulate α-cell Ca^{2+}. Consistently, the application of small molecule PK activators (10 μM TEPP-46), which allosterically activate PKM2 and PKL to drive the PEP cycle [34,36,38], nearly abolished the Ca^{2+} response to an amino acid ramp (Figure 4A). To confirm that this effect was due to a direct effect on the α-cell, we applied the same amino acid ramp to islets isolated from PKM1/2-αKO and PCK2-αKO mice. Control islets were again measured simultaneously using islet barcoding. Elevated α-cell Ca^{2+} was observed in response to a range of amino acid levels in both PKM1/2-αKO and PCK2-αKO islets relative to controls (Figure 4B,C). As in the electrophysiological assays, α-cell deletion of PCK2 had a stronger effect on Ca^{2+} levels than deletion of PKM1/2. Taking advantage of this phenotype, we used PCK2-αKO islets to test effects of individual amino acids on Ca^{2+} levels (Supplemental Figure 3). Alanine and arginine were able to stimulate Ca^{2+} influx regardless of whether glutamine and leucine are present, as expected for their direct role in controlling V_m. However, the Ca^{2+} phenotype of the PCK2-αKO islets was lost in the absence of glutamine, consistent with its role in providing anaplerotic glutamate carbons that drive oxaloacetate formation for PCK2. These data indicate that the α-cell PEP cycle cannot function in experiments lacking glutamine.

We next investigated whether Ca^{2+} regulation by the PEP cycle impacts glucagon secretion using islet perfusion assays. Amino acids and GIP were sequentially applied under low glucose conditions to maximally stimulate glucagon release. However, we observed no difference in glucagon release upon PK activation with TEPP-46 (Figure 4D), or upon α-cell deletion of PKM1/2 or PCK2 (Figure 4E,F). Similar results were obtained in PCK2-αKO islets and controls were stimulated with alanine and GIP in the absence of leucine (Supplemental Figure 4). The enhanced intracellular Ca^{2+} levels observed in α-cells lacking PKM1/2 and PCK2 is consistent with the permissive role of Ca^{2+} in controlling glucagon release. The ability of PK activation to suppress amino acid stimulated Ca^{2+} influx without impacting secretion not only indicates that Ca^{2+} influx at 2 mM glucose is sufficient to trigger glucagon secretion, but that amino acid stimulation of Ca^{2+} influx has no bearing on secretion.

Changes in cytosolic Ca^{2+} can also be modulated by Ca^{2+} extrusion. To test for a role of the PEP cycle downstream of V_m depolarization, we performed experiments in the presence of the K_{ATP} channel opener diazoxide (200 μM) and then triggered Ca^{2+} influx with 30 mM KCl. Even

with V_m clamped, Ca^{2+} reached a higher level in α-cells lacking PKM1/2 or PCK2 (Figure 4G,H). These findings indicate that the α-cell PEP cycle, in addition to controlling V_m, homeostatically suppresses intracellular Ca^{2+} levels after glucagon is released.

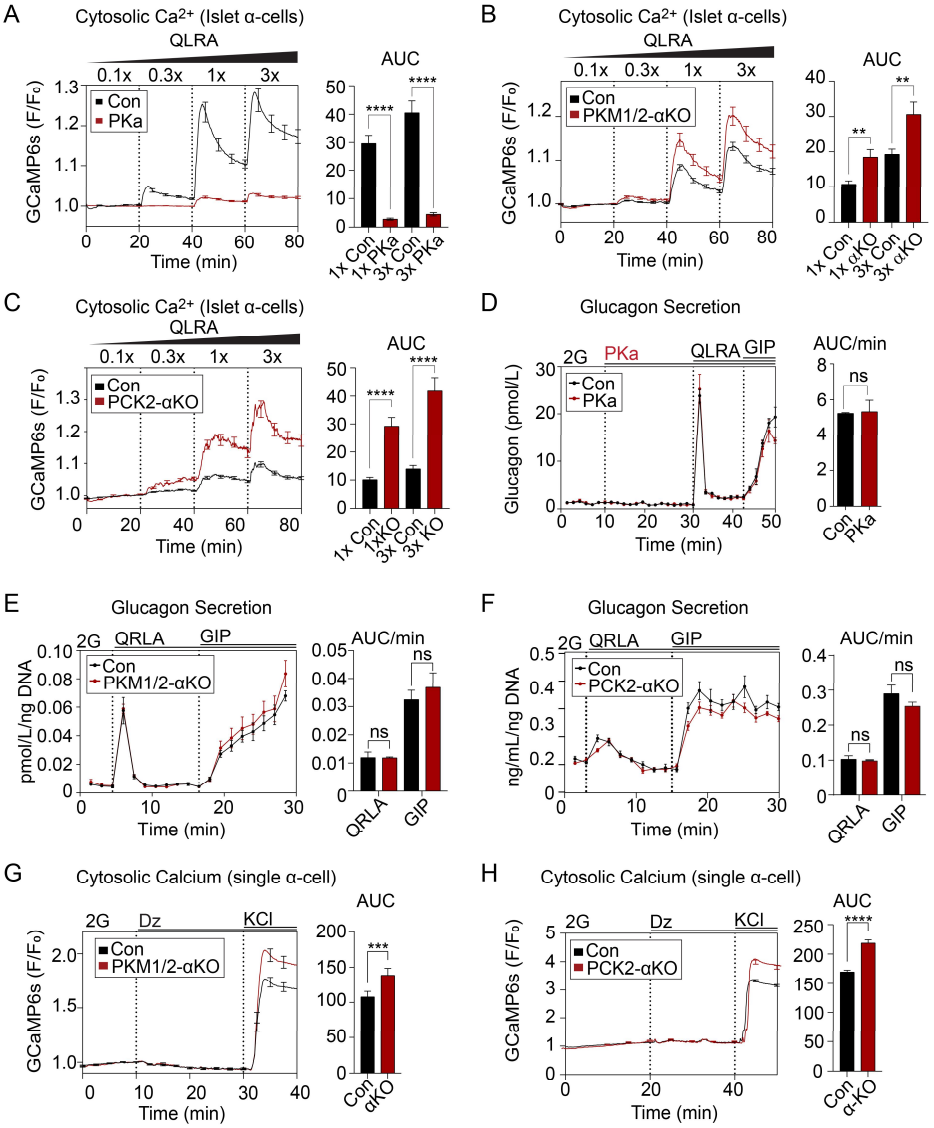

Figure 4. Pyruvate kinase and PCK2 suppress α-cell Ca^{2+} without impacting glucagon secretion. (A-C) Average α-cell Ca^{2+} in response to amino acid ramp (1x QLRA; 0.6 mM glutamine, 0.5 mM leucine, 0.2 mM arginine, 2 mM and alanine) in islets from α-cell GCaMP6s mice treated with pyruvate kinase activator (PKa, 10μM TEPP-46), islets from control and PKM1/2-αKO mice (B), or control and PCK2-αKO mice (C). Data represent 57-105 islets from 3 mice per group. (D-E) Average α-cell Ca^{2+} in response to 200 μM diazoxide followed by 30 mM KCl in intact islets from control and PKM1/2-αKO (D) and PCK2-αKO mice (E). Data represent 904-1194 α-cells from 4 mice. (F-H) Glucagon secretion in response to QLRA, GIP (10 nM) in wild-type mice treated with PKa (F), control and PKM1/2-αKO mice (G), or control and PCK2-αKO mice (H). Data represent 6 chambers from 6 mice per condition with 80–100 mouse islets per chamber. Data are shown as mean ± SEM with AUC for each condition compared with control by Student's *t* test. $^{**}P < 0.01$, $^{***}P < 0.001$, $^{****}P < 0.0001$, ns, not significant.

3. Discussion

Our data provide strong support for the concept of α-cells as amino acids sensors [3]. We confirmed that alanine and arginine stimulate Ca^{2+} influx and glucagon secretion at physiological concentrations. Glutamine and leucine, while having only a small effect on Ca^{2+} at low glucose, strongly antagonized alanine/arginine-stimulated V_m depolarization and Ca^{2+} influx. We used three different models to show that glutamine and leucine suppress Ca^{2+} via α-cell PEP cycle, including pharmacological PK activators and α-cell specific deletion of PKM1/2 and PCK2. Strikingly, all three of these manipulations modulated Ca^{2+} without changing glucagon secretion. Thus, the glucagon released in response to amino acids, including electrogenic alanine and arginine, is not dependent on their ability to stimulate Ca^{2+} influx.

At the mechanistic level, we found that both PCK2 and PK are required for glutamine/leucine to close K_{ATP} channels, mirroring findings in β-cells [18,34–36], but the functional outcomes are different. While β-cells use the PEP cycle to initiate secretion, α-cells use it primarily to modulate Ca^{2+} dynamics. Specifically, we provided genetic evidence that PK is involved in suppressing intracellular Ca^{2+} levels in response to mitochondrial fuels. Part of this effect may arise from the ability of PK to close K_{ATP} channels and suppress membrane depolarization. These findings are consistent with our prior report indicating that a glycolytic metabolon is present on the plasma membrane of islet cells, and regulates α-cell K_{ATP} channels via the ATP/ADP ratio [18]. Similar to glycolysis, mitochondrial PCK2 can generate PEP in response to glutamine/leucine. Deletion of PCK2 or PKM1/2 in α-cells blocked K_{ATP} closure in response to glutamine/leucine, indicating a conserved pathway in both α and β-cells [35]. Of course, K_{ATP} closure has different effects on electrical excitability in α- and β-cells [11]. In α-cells, we observed that both membrane potential and Ca^{2+} levels increased in response to amino acid stimulation in the PCK2 and PKM1/2 deletion models. In addition to K_{ATP} channels, there are other potential mechanisms of V_m regulation that we did not explore, such as metabolic control of α-cell Na^+/K^+ ATPases [39], which facilitate V_m hyperpolarization in β-cells [40].

Several factors may explain why elevated Ca^{2+} in our knockout models failed to enhance secretion. First is that Ca^{2+} is only permissive for hormone secretion in islet cells [6,41]. From this perspective, it makes sense that elevated Ca^{2+} in the PCK2-αKO and PKM1/2-αKO has little impact on glucagon secretion, particularly in the presence of arginine and alanine that strongly stimulate Ca^{2+}. Previous findings show that glucagon release is largely controlled by mouse α-cell P/Q-type Ca^{2+} channels, although they only account for ~20% of Ca^{2+} current [10]. Second, since glucagon release is not changed by PK or the PEP cycle, it is possible that K_{ATP} channels primarily impact L-type VDCC, as in β-cells. In any case, the field must look beyond Ca^{2+} to understand amino acid regulation of glucagon secretion. The glucagonostatic effect of leucine is both Ca^{2+}- and PEP cycle-independent, and may be primarily mediated by its ability to reduce cAMP [31]. Of note, gain-of-function mutations in glutamate dehydrogenase cause hyperinsulinemic hypoglycemia in response to protein rich meals [42]. We believe this effect is due to glutamine carbons funneling through PCK2 and PK to close K_{ATP} channels [43]. However, in α-cells, a change in glucagon secretion is not observed even when flux through PEP cycle is increased, potentially explaining why glutamate dehydrogenase mutations do not impact glucagon secretion.

Importantly, the elevated levels of Ca^{2+} in the knockout models were also observed in the presence of diazoxide/KCl, which stimulates Ca^{2+} influx independently of K_{ATP} closure. These findings indicate that the PEP cycle restores intracellular Ca^{2+} levels after depolarization. In cell

291 lines, PK has been previously shown to play a role in ER Ca^{2+} storage [44]. At low glucose, and
292 in the absence of fatty acids [17], glutamine/leucine are key mitochondrial substrates. Defects in
293 metabolism induced by α-cell PKM1/2 and PCK2 deletion could therefore impair Ca^{2+} extrusion.
294 Mitochondria are also important for Ca^{2+} sequestration [45]. In β-cells, the PEP cycle has been
295 shown to hyperpolarize the mitochondrial membrane as PK lowers ADP (i.e., ADP privation) [34],
296 and could affect mitochondrial Ca^{2+} handling. Further studies are needed to understand how amino
297 acids affect organellar Ca^{2+} handling. In the meantime, our work shows that α-cells use the PEP
298 cycle not as a direct regulator of secretion, but rather to the limit Ca^{2+} rise during amino acid
299 stimulation.
300

301 **4. Material and methods**

302 *4.1. Mice*

303 Wild-type C57BL/6J mice were obtained from The Jackson Laboratory. *GcgCre^{ERT}* mice (Jax
304 030346) [46] were crossed with *GCaMP6s* mice (Jax 028866), a Cre-dependent Ca^{2+} indicator
305 strain. *Pkm$^{f/f}$* mice were generated using CRISPR and sequence-verified by the University of
306 Wisconsin-Madison Genome Editing and Animal Model Core, as done previously to generate
307 *Pck2$^{f/f}$* mice [35]. *Pkm$^{f/f}$* and *Pck2$^{f/f}$* mice were crossed with *GcgCre^{ERT}:GCaMP6s* mice to generate
308 *GcgCre^{ERT}:GCaMP6s:Pkm$^{f/f}$* (PKM1/2-αKO) and *GcgCre^{ERT}:GCaMP6s:Pck2$^{f/f}$* (PCK2-αKO) and
309 their littermate *GcgCre^{ERT}:GCaMP6s* controls. As in our prior study, *GcgCre^{ERT}* was present in the
310 dams to facilitate *loxP* excision in the study animals without the need for tamoxifen [31]. Mice
311 were used between 11-24 weeks of age. Although 4-hydroxytamoxifen (100 nM) was only strictly
312 necessary for adenoviral expression of Cre-dependent JEDI-2P biosensors, it was included in the
313 culture media in all islet studies for consistency, after verifying that hormone secretion was
314 unaffected (Supplemental Figure 6). All procedures involving animals were approved by the
315 Institutional Animal Care and Use Committees of the William S. Middleton Memorial Veterans
316 Hospital and the University of Wisconsin-Madison and followed the National Institutes of Health
317 Guide for the Care and Use of Laboratory Animals.
318

319 *4.2. In vivo assays*

320 For meal tolerance tests, mice were fasted for 5 hours prior to oral gavage of liquid Ensure (10
321 mL/kg). For insulin tolerance tests, animals were fasted for 5 hours, followed by IP-injection of
322 0.75 mg/kg Humilin-R (Eli Lilly). Blood glucose was measured from the tail using a glucometer
323 (Contour). Glucagon was assayed from blood plasma using a mouse glucagon ELISA kit (Crystal
324 Chem 81518) assayed with a TECAN Spark plate reader.
325

326 *4.3. Islet Perifusion Assays*

327 Islets from 5-6 mice of each genotype were pooled and then divided in equal numbers (80-100
328 islets/chamber) and placed into a 12-channel perifusion system (BioRep Peri-5 or homemade
329 perifusion system) containing KRPH buffer (in mM: 140 NaCl, 4.7 KCl, 2.5 $CaCl_2$, 1 NaH_2PO_4,
330 1 $MgSO_4$, 2 $NaHCO_3$, 5 HEPES, 2 glucose, 0.1% fatty acid-free BSA, pH 7.4) using 100 µL Bio-
331 Gel P-4 Media (Bio-Rad #1504124) to stabilize the islets. Islets were equilibrated at 2 mM glucose
332 for 48 min prior to perfusion with AA at 37°C. Glucagon secretion was assayed using Promega
333 Lumit Glucagon Immunoassay (W8020) and measured using a TECAN Spark plate reader. The

Quant-IT PicoGreen dsDNA Assay Kit (Invitrogen P7589) was used to determine DNA content after lysis in 0.1% Triton X-100.

4.4. Immunofluorescence staining and quantification

Isolated islets were fixed in 4% paraformaldehyde, permeabilized in CAS-Block (Invitrogen) containing 0.3% Triton X-100 for 1 hour at room temperature, and subsequently incubated overnight at 4°C with primary antibodies diluted in CAS-Block/Triton: rabbit-anti-PKM1/2 (CST3190T, 1:200); rabbit-anti-PCK2 (CST6924S, 1:200); mouse-anti-glucagon (ab10988, 1:800). Following five 10-minute washes in PBST (PBS with 0.1% Triton X-100), islets were incubated with secondary antibodies (Abberior STAR Orange anti-mouse and STAR Red anti-rabbit, 1:200) for 4 hours at room temperature, followed by five 10-minute PBST washes. Stained islets were mounted on glass slides using ProLong Gold Antifade (Invitrogen) and imaged on a Nikon AXR NSPARC confocal microscope. Z-stacks were acquired at 1 µm step size, covering 10-30 planes per islet. For quantification, glucagon signal was used to define α-cell vs. non-α-cell regions of interest (ROI). Whole-cell PKM1/2 and PCK2 staining intensities were measured within randomly selected ROIs across z-planes and islets. Statistical comparisons were performed using ordinary one-way ANOVA.

4.5. FACS sorting and qPCR

Islets isolated from 6mice/group were pooled and dispersed with trypsin (TrypLE, Thermo fisher). Cells were sorted using FACSAriaII at University of Wisconsin Carbone Cancer Center Flow Lab. α and non α-cells were sorted based on GCaMP6s signal. RNA was isolated using QIAGEN RNeasy mini kit according to the manufacturer's instructions. cDNA was prepared using monkey Moloney virus reverse transcriptase (Life Technologies) then analyzed by quantitative PCR (qPCR) using Power SYBR Master Mix (Life Technologies)(Forward primer: TGGCCGTGCAATCCAGAAAA; Reverse primer: TTGGTGATGCCCAAAATCAGCAT). All transcripts were normalized to β-actin. Fold changes were calculated relative to vehicle only controls.

4.6. Electrophysiology

Mouse islets were dispersed with Accutase (Sigma-Aldrich A6964100ML) and plated on sterilized uncoated glass shards and cultured for up to 3 days. Recording electrodes made of microfilament borosilicate glass (Harvard Apparatus) were used to pull ~3 MΩ patch pipettes using a Flaming/Brown micropipette puller (P-1000, Sutter Instruments), and polished (Narishige MF-830) to a final tip resistance of 4-5 MΩ. Cell-attached recording started after formation of a stable gigaseal (>3 GΩ). Recordings were made by using HEKA Instruments EPC10 patch-clamp amplifier at room temperature. The pipette solution contained (in mM): 10 sucrose, 130 KCl, 2 $CaCl_2$, 0.9 $MgCl_2$, 10 EGTA, 20 HEPES, pH 7.2, adjusted with KOH. The extracellular bath solution contained (in mM): 140 NaCl, 5 KCl, 1.2 $MgCl_2$, 2.5 $CaCl_2$, 0.5 glucose, 10 HEPES, pH 7.4, adjusted with NaOH. Holding membrane potential was set at −50 mV during recording. Data was filtered online at 1 kHz with a Bessel filter and analyzed offline using Clampfit 10.7 software (Molecular Devices). During each condition, recordings are held for several minutes for the activity to stabilize, such that no significant further changes in channel conductance were observed. A 120-s window at the end of each condition was used to analyze K_{ATP} activity in terms of power, frequency, and duration and open time as previously described [18], all of which were normalized

379 to control conditions. Membrane potential measurement was performed as in[47]. Briefly, Intact
380 islets were perfused with a standard external solution containing (135 mM NaCl, 4.8 mM KCl,
381 5 mM $CaCl_2$, 1.2 mM $MgCl_2$, 20 mM HEPES, 10 mM glucose; pH 7.35) with 2mM glucose and
382 amino acids as indicated. Pipette tips were filled with an internal solution (28.4 mM K_2SO_4,
383 63.7 mM KCl, 11.8 mM NaCl, 1 mM $MgCl_2$, 20.8 mM HEPES, 0.5 mM EGTA; 40 mM sucrose;
384 pH 7.2) containing 0.36 mg/mL amphotericin B. Islet α and β-cells were identified by their
385 characteristic I-V curves (Supplemental Figure 3)
386
387 *4.7. Islet Ca^{2+} and V_m imaging*
388 Reagents were obtained from Sigma-Aldrich unless indicated otherwise. For imaging of α-cell
389 Ca^{2+}, islets isolated from *GcgCre^{ERT}:GCaMP6s* mice were cultured in the presence of 100 nM 4-
390 hydroxytamoxifen and imaged 3 days post isolation. Islets with different genotypes were barcoded
391 by preincubation with 2 μM DiR (Thermo Fisher Scientific D12731) in 2ml islet media for 15 min
392 at 37°C. Islet barcode was then imaged using Cy7 (for DiR) from Chroma. For imaging of α-cell
393 membrane potential, islets from *GcgCre^{ERT}* mice were incubated with adenovirus expressing Cre-
394 dependent JEDI-2P biosensors (Ad-CMV-FlexOn-JEDI-2P, VectorBuilder) for 2 hours, transferred
395 to fresh media containing 100 nM 4-hydroxytamoxifen, and imaged 3 days post isolation. Islets
396 were imaged on an RC-41LP chamber (Warner Instruments) mounted on a Nikon Ti2 microscope
397 equipped with a 10×/0.5 NA SuperFluor objective (Nikon). The imaging solution contained (in
398 mM): 137 NaCl, 5.6 KCl, 1.2 $MgCl_2$, 0.5 NaH_2PO_4, 4.2 $NaHCO_3$, 10 HEPES, and 2.6 $CaCl_2$ (pH
399 7.4). Metabolites, mouse GIP (Pheonix Pharmaceuticals), and pyruvate kinase activator (TEPP-
400 46, Calbiochem) were added as indicated. Islets were imaged at a constant flow rate of 250 μL/min
401 using a feedback-controlled flow cell (Fluigent) and the temperature was maintained at 37°C with
402 chamber and solution heaters (Warner). Filters for GCAMP6s and JEDI-2P imaging were as
403 follows: exciter, ET500/20x; dichroic, ET-Fura2-GFP; emitter, ET535/30m (Chroma). Images
404 were captured with a Hamamatsu ORCA-Flash4.0 CMOS camera every 6 s. A single region of
405 interest was used to quantify the average response of each islet using NIS-Elements software
406 (Nikon Instruments). Ca^{2+} and membrane potential were reported as the fluorescence intensity
407 normalized to the initial condition (F/F_o). Single α-cell quantification was performed with the
408 Imaris analysis software (Oxford Instruments).
409
410 **CRediT authorship contribution statement**
411 **Erli Jin:** Conceptualization, Writing – original draft, Writing – review & editing, Methodology,
412 Investigation, Formal analysis. **Hannah R. Foster**: Methodology, Investigation, Formal analysis.
413 **Evgeniy Potapenko**: Methodology, Investigation, Formal analysis. **Shih Ming Huang**:
414 Methodology, Investigation. **Xinhang Dong**: Methodology, Investigation, Formal analysis. **Jing**
415 **W. Hughes**: Methodology, Investigation, Formal analysis, Writing – review & editing. **Matthew**
416 **J. Merrins**: Writing – original draft, Writing – review & editing, Supervision, Conceptualization,
417 Funding acquisition.
418
419 **Acknowledgements**
420 The Merrins laboratory gratefully acknowledges support from the NIH/NIDDK (R01DK113103
421 and R01DK127637 to M.J.M.) and the United States Department of Veterans Affairs Biomedical

Laboratory Research and Development Service (I01BX005113 to M.J.M.). The Hughes laboratory gratefully acknowledges support from the NIH DK138974 and DK140365 to JWH.

Appendix A. Supplementary data

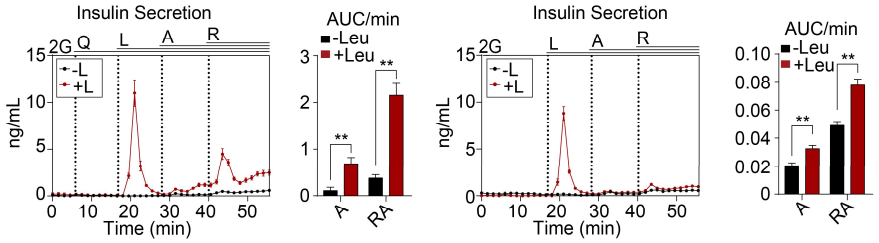

Supplemental Figure 1. Leucine stimulates insulin secretion at low glucose. Insulin secretion from mouse islets measured as in Figure 1I-J. Data are shown as mean ± SEM with AUC for each condition compared with control by Student's *t* test. $^{**}P < 0.01$.

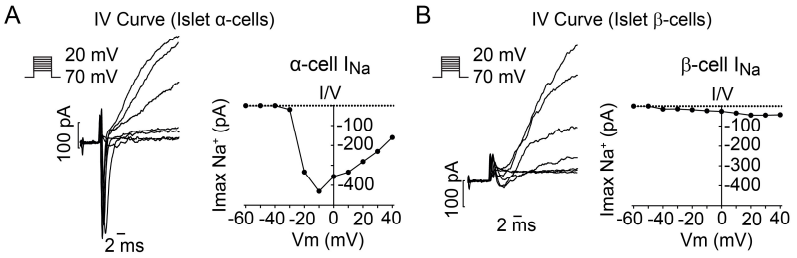

Supplemental Figure 2. I–V curves used for α-cell identification in intact islets. Example traces and I-V curves measured from surface α-cells (A) and β-cells (B) in bath solution containing 2 mM glucose and 0.5 mM glutamine. Cells were depolarized from a holding potential of -70 mV to voltages between −60 and +40 mV in 10 mV increments. Data represent 12-18 cells from 3 mice per group as in Figure 3C-D.

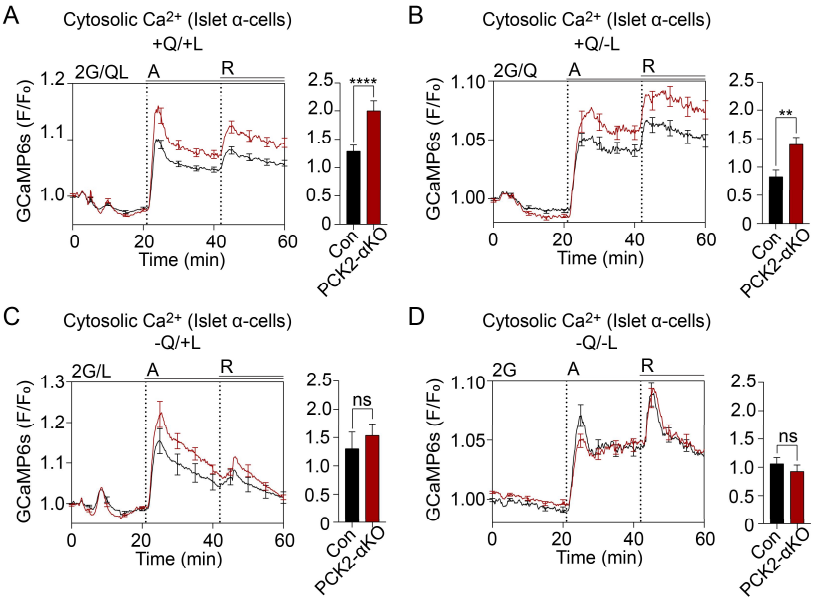

Supplemental Figure 3. The α-cell Ca^{2+} PEP cycle requires glutamine. (A-D) Averaged Ca^{2+} from control and PCK2-αKO mice in response to 2 mM glucose and combinations of amino acids as indicated. Data represent 42-55 islets from 3 mice per group. Data are shown as mean ± SEM with AUC for each condition compared with control by Student's *t* test. $^{**}P < 0.01$, $^{****}P < 0.0001$, ns, not significant.

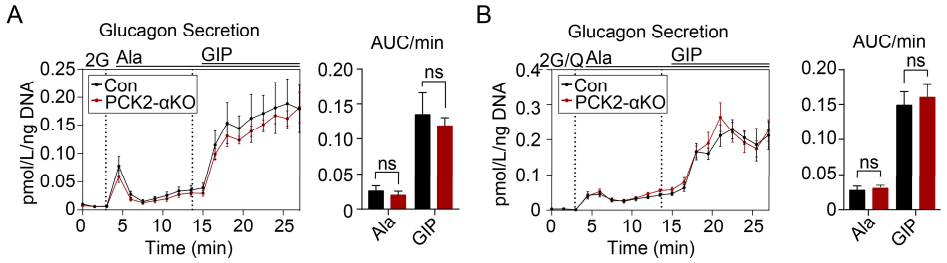

Supplemental Figure 4. The α-cell Ca^{2+} PEP cycle is not required for glucagon secretion stimulated by alanine and GIP. Glucagon secretion control and PCK2-αKO islets in response to alanine (2 mM) and GIP (10 nM GIP). Data represent 3-6 chambers from 3-5 mice per condition with 80–100 mouse islets per chamber. Data are shown as mean ± SEM with AUC for each condition compared with control by Student's *t* test. ns, not significant.

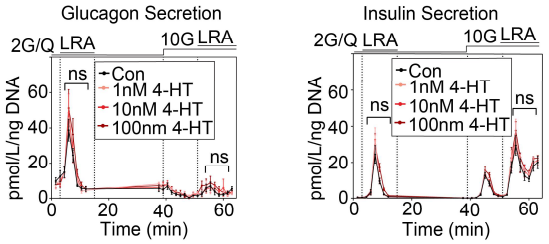

Supplemental Figure 5. Culturing mouse islets 4-hydroxytamoxifen does not impact glucagon and insulin secretion. Hormone secretion measured from mouse islets after 3-day treatment with 1, 10, and 100 nM 4-hydroxytamoxifen (4-HT) in the culture media. Islets were measured in the presence of glucose (2G: 2mM glucose; 10G: 10mM glucose) and amino acids as indicated (QLRA, in mM: 0.6 mM glutamine, 0.5 mM leucine, 0.2 mM arginine, 2 mM and alanine). Data represent the average of 3 chambers from 3 mice per condition with 80 mouse islets per chamber. Data are shown as mean ± SEM with AUC for each condition compared with control by 2-way ANOVA. ns, not significant.

Reference

[1] Capozzi, M.E., D'Alessio, D.A., Campbell, J.E., 2022. The past, present, and future physiology and pharmacology of glucagon. Cell Metabolism 34(11): 1654–74, Doi: 10.1016/j.cmet.2022.10.001.

[2] Armour, S.L., Stanley, J.E., Cantley, J., Dean, E.D., Knudsen, J.G., 2023. Metabolic regulation of glucagon secretion. The Journal of Endocrinology: JOE-23-0081, Doi: 10.1530/JOE-23-0081.

465 [3] Dean, E.D., 2020. A Primary Role for α-Cells as Amino Acid Sensors. Diabetes 69(4):
466 542–9, Doi: 10.2337/dbi19-0021.

467 [4] Hamilton, A., Eliasson, L., Knudsen, J.G., 2023. Amino acids and the changing face of
468 the α-cell. Peptides 166: 171039, Doi: 10.1016/j.peptides.2023.171039.

469 [5] Gilon, P., 2020. The Role of α-Cells in Islet Function and Glucose Homeostasis in Health
470 and Type 2 Diabetes. Journal of Molecular Biology 432(5): 1367–94, Doi:
471 10.1016/j.jmb.2020.01.004.

472 [6] Le Marchand, S.J., Piston, D.W., 2012. Glucose Decouples Intracellular Ca2+ Activity
473 from Glucagon Secretion in Mouse Pancreatic Islet Alpha-Cells. PLoS ONE 7(10): e47084, Doi:
474 10.1371/journal.pone.0047084.

475 [7] Onyango, A.N., 2020. Mechanisms of the Regulation and Dysregulation of Glucagon
476 Secretion. Oxidative Medicine and Cellular Longevity 2020: 3089139, Doi:
477 10.1155/2020/3089139.

478 [8] Dai, X.-Q., Camunas-Soler, J., Briant, L.J.B., Santos, T., Spigelman, A.F., Walker, E.M.,
479 et al., 2022. Heterogenous impairment of α cell function in type 2 diabetes is linked to cell
480 maturation state. Cell Metabolism 34(2): 256-268.e5, Doi: 10.1016/j.cmet.2021.12.021.

481 [9] Acreman, S., Ma, J., Denwood, G., Gao, R., Tarasov, A., Rorsman, P., et al., 2024. The
482 endoplasmic reticulum plays a key role in α-cell intracellular Ca2+ dynamics and glucose-
483 regulated glucagon secretion in mouse islets. iScience 27(5): 109665, Doi:
484 10.1016/j.isci.2024.109665.

485 [10] Zhang, Q., Ramracheya, R., Lahmann, C., Tarasov, A., Bengtsson, M., Braha, O., et al.,
486 2013. Role of KATP Channels in Glucose-Regulated Glucagon Secretion and Impaired
487 Counterregulation in Type 2 Diabetes. Cell Metabolism 18(6): 871–82, Doi:
488 10.1016/j.cmet.2013.10.014.

489 [11] Zhang, Q., Dou, H., Rorsman, P., 2020. 'Resistance is futile?' – paradoxical inhibitory
490 effects of K_{ATP} channel closure in glucagon-secreting α-cells. The Journal of Physiology
491 598(21): 4765–80, Doi: 10.1113/JP279775.

492 [12] Gromada, J., Ma, X., Høy, M., Bokvist, K., Salehi, A., Berggren, P.-O., et al., 2004. ATP-
493 Sensitive K+ Channel–Dependent Regulation of Glucagon Release and Electrical Activity by
494 Glucose in Wild-Type and *SUR1* −/− Mouse α-Cells. Diabetes 53(suppl_3): S181–9, Doi:
495 10.2337/diabetes.53.suppl_3.S181.

496 [13] Briant, L.J.B., Dodd, M.S., Chibalina, M.V., Rorsman, N.J.G., Johnson, P.R.V.,
497 Carmeliet, P., et al., 2018. CPT1a-Dependent Long-Chain Fatty Acid Oxidation Contributes to
498 Maintaining Glucagon Secretion from Pancreatic Islets. Cell Reports 23(11): 3300–11, Doi:
499 10.1016/j.celrep.2018.05.035.

[14] Armour, S.L., Frueh, A., Chibalina, M.V., Dou, H., Argemi-Muntadas, L., Hamiltion, A., et al., 2023. Glucose controls glucagon secretion by regulating fatty acid oxidation in pancreatic alpha cells. Diabetes: db230056, Doi: 10.2337/db23-0056.

[15] Ramracheya, R., Ward, C., Shigeto, M., Walker, J.N., Amisten, S., Zhang, Q., et al., 2010. Membrane potential-dependent inactivation of voltage-gated ion channels in alpha-cells inhibits glucagon secretion from human islets. Diabetes 59(9): 2198–208, Doi: 10.2337/db09-1505.

[16] MacDonald, P.E., Marinis, Y.Z.D., Ramracheya, R., Salehi, A., Ma, X., Johnson, P.R.V., et al., 2007. A KATP Channel-Dependent Pathway within α Cells Regulates Glucagon Release from Both Rodent and Human Islets of Langerhans. PLoS Biology 5(6): e143, Doi: 10.1371/journal.pbio.0050143.

[17] Armour, S.L., Frueh, A., Chibalina, M.V., Dou, H., Argemi-Muntadas, L., Hamilton, A., et al., 2023. Glucose Controls Glucagon Secretion by Regulating Fatty Acid Oxidation in Pancreatic α-Cells. Diabetes 72(10): 1446–59, Doi: 10.2337/db23-0056.

[18] Ho, T., Potapenko, E., Davis, D.B., Merrins, M.J., 2023. A plasma membrane-associated glycolytic metabolon is functionally coupled to KATP channels in pancreatic α and β cells from humans and mice. Cell Reports 42(4): 112394, Doi: 10.1016/j.celrep.2023.112394.

[19] Bahl, V., Rifkind, R., Waite, E., Hamdan, Z., May, C.L., Manduchi, E., et al., 2025. G6PC2 controls glucagon secretion by defining the set point for glucose in pancreatic α cells. Science Translational Medicine 17(779): eadi6148, Doi: 10.1126/scitranslmed.adi6148.

[20] Bahl, V., Lee May, C., Perez, A., Glaser, B., Kaestner, K.H., 2021. Genetic activation of α-cell glucokinase in mice causes enhanced glucose-suppression of glucagon secretion during normal and diabetic states. Molecular Metabolism 49: 101193, Doi: 10.1016/j.molmet.2021.101193.

[21] Cabrera, O., Jacques-Silva, M.C., Speier, S., Yang, S.-N., Köhler, M., Fachado, A., et al., 2008. Glutamate Is a Positive Autocrine Signal for Glucagon Release. Cell Metabolism 7(6): 545–54, Doi: 10.1016/j.cmet.2008.03.004.

[22] Li, C., Liu, C., Nissim, I., Chen, J., Chen, P., Doliba, N., et al., 2013. Regulation of glucagon secretion in normal and diabetic human islets by γ-hydroxybutyrate and glycine. The Journal of Biological Chemistry 288(6): 3938–51, Doi: 10.1074/jbc.M112.385682.

[23] Zhang, Z., Ye, W.W., Piro, A.L., Wang, D.-S., Untereiner, A., Lyons, S.A., et al., n.d. Glycine receptor activation promotes pancreatic islet cell proliferation via the PI3K/mTORC1/p70S6K pathway. JCI Insight 10(8): e178754, Doi: 10.1172/jci.insight.178754.

[24] Malaisse, W.J., Blachier, F., Mourtada, A., Camara, J., Albor, A., Valverde, I., et al., 1989. Stimulus-secretion coupling of arginine-induced insulin release. Metabolism of l-arginine and l-

534 ornithine in pancreatic islets. Biochimica et Biophysica Acta (BBA) - Molecular Cell Research
535 1013(2): 133–43, Doi: 10.1016/0167-4889(89)90041-4.

536 [25] Spears, E., Stanley, J.E., Shou, M., Yin, L., Li, X., Dai, C., et al., 2023. Pancreatic islet α
537 cell function and proliferation requires the arginine transporter SLC7A2: 2023.08.10.552656,
538 Doi: 10.1101/2023.08.10.552656.

539 [26] El, K., Gray, S.M., Capozzi, M.E., Knuth, E.R., Jin, E., Svendsen, B., et al., 2021. GIP
540 mediates the incretin effect and glucose tolerance by dual actions on α cells and β cells. Science
541 Advances 7(11): eabf1948, Doi: 10.1126/sciadv.abf1948.

542 [27] Simmons, T.W., Moseley, R.H., Boyer, J.L., Ballatori, N., 1990. Modulation of
543 Na+/alanine cotransport in liver sinusoidal membrane vesicles by internal divalent cations.
544 Biochimica et Biophysica Acta (BBA) - Biomembranes 1023(3): 462–8, Doi: 10.1016/0005-
545 2736(90)90140-J.

546 [28] Rocha, D.M., Faloona, G.R., Unger, R.H., 1972. Glucagon-stimulating activity of 20
547 amino acids in dogs. Journal of Clinical Investigation 51(9): 2346–51, Doi: 10.1172/JCI107046.

548 [29] Li, C., Najafi, H., Daikhin, Y., Nissim, I.B., Collins, H.W., Yudkoff, M., et al., 2003.
549 Regulation of leucine-stimulated insulin secretion and glutamine metabolism in isolated rat
550 islets. The Journal of Biological Chemistry 278(5): 2853–8, Doi: 10.1074/jbc.M210577200.

551 [30] Sener, A., Malaisse, W.J., 1980. L-leucine and a nonmetabolized analogue activate
552 pancreatic islet glutamate dehydrogenase. Nature 288(5787): 187–9, Doi: 10.1038/288187a0.

553 [31] Knuth, E.R., Foster, H.R., Jin, E., Ekstrand, M.H., Knudsen, J.G., Merrins, M.J., 2024.
554 Leucine Suppresses α-Cell cAMP and Glucagon Secretion via a Combination of Cell-Intrinsic
555 and Islet Paracrine Signaling. Diabetes 73(9): 1426–39, Doi: 10.2337/db23-1013.

556 [32] Dean, E.D., Li, M., Prasad, N., Wisniewski, S.N., Von Deylen, A., Spaeth, J., et al., 2017.
557 Interrupted Glucagon Signaling Reveals Hepatic α Cell Axis and Role for L-Glutamine in α Cell
558 Proliferation. Cell Metabolism 25(6): 1362-1373.e5, Doi: 10.1016/j.cmet.2017.05.011.

559 [33] Armour, S.L., Stanley, J.E., Cantley, J., Dean, E.D., Knudsen, J.G., 2023. Metabolic
560 regulation of glucagon secretion. The Journal of Endocrinology 259(1): e230081, Doi:
561 10.1530/JOE-23-0081.

562 [34] Lewandowski, S.L., Cardone, R.L., Foster, H.R., Ho, T., Potapenko, E., Poudel, C., et al.,
563 2020. Pyruvate Kinase Controls Signal Strength in the Insulin Secretory Pathway. Cell
564 Metabolism 32(5): 736-750.e5, Doi: 10.1016/j.cmet.2020.10.007.

565 [35] Foster, H.R., Ho, T., Potapenko, E., Sdao, S.M., Huang, S.M., Lewandowski, S.L., et al.,
566 2022. β-cell deletion of the PKm1 and PKm2 isoforms of pyruvate kinase in mice reveals their
567 essential role as nutrient sensors for the KATP channel. eLife 11: e79422, Doi:
568 10.7554/eLife.79422.

[36] Abulizi, A., Cardone, R.L., Stark, R., Lewandowski, S.L., Zhao, X., Hillion, J., et al., 2020. Multi-Tissue Acceleration of the Mitochondrial Phosphoenolpyruvate Cycle Improves Whole-Body Metabolic Health. Cell Metabolism 32(5): 751-766.e11, Doi: 10.1016/j.cmet.2020.10.006.

[37] Liu, Z., Lu, X., Villette, V., Gou, Y., Colbert, K.L., Lai, S., et al., 2022. Sustained deep-tissue voltage recording using a fast indicator evolved for two-photon microscopy. Cell 185(18): 3408-3425.e29, Doi: 10.1016/j.cell.2022.07.013.

[38] Anastasiou, D., Yu, Y., Israelsen, W.J., Jiang, J.-K., Boxer, M.B., Hong, B.S., et al., 2012. Pyruvate kinase M2 activators promote tetramer formation and suppress tumorigenesis. Nature Chemical Biology 8(10): 839–47, Doi: 10.1038/nchembio.1060.

[39] Barg, S., Galvanovskis, J., Göpel, S.O., Rorsman, P., Eliasson, L., 2000. Tight coupling between electrical activity and exocytosis in mouse glucagon-secreting alpha-cells. Diabetes 49(9): 1500–10, Doi: 10.2337/diabetes.49.9.1500.

[40] Dickerson, M.T., Dadi, P.K., Zaborska, K.E., Nakhe, A.Y., Schaub, C.M., Dobson, J.R., et al., 2022. Gi/o protein-coupled receptor inhibition of beta-cell electrical excitability and insulin secretion depends on Na+/K+ ATPase activation. Nature Communications 13(1): 6461, Doi: 10.1038/s41467-022-34166-z.

[41] Hughes, J.W., Ustione, A., Lavagnino, Z., Piston, D.W., 2018. Regulation of islet glucagon secretion: Beyond calcium. Diabetes, Obesity & Metabolism 20 Suppl 2: 127–36, Doi: 10.1111/dom.13381.

[42] Luczkowska, K., Stekelenburg, C., Sloan-Béna, F., Ranza, E., Gastaldi, G., Schwitzgebel, V., et al., 2020. Hyperinsulinism associated with GLUD1 mutation: allosteric regulation and functional characterization of p.G446V glutamate dehydrogenase. Human Genomics 14: 9, Doi: 10.1186/s40246-020-00262-8.

[43] Merrins, M.J., Kibbey, R.G., 2024. Glucose Regulation of β-Cell KATP Channels: It Is Time for a New Model! Diabetes 73(6): 856–63, Doi: 10.2337/dbi23-0032.

[44] Ho, P.-C., Bihuniak, J.D., Macintyre, A.N., Staron, M., Liu, X., Amezquita, R., et al., 2015. Phosphoenolpyruvate Is a Metabolic Checkpoint of Anti-tumor T Cell Responses. Cell 162(6): 1217–28, Doi: 10.1016/j.cell.2015.08.012.

[45] Griesche, N., Sanchez, G., Hermans, C., Idevall-Hagren, O., 2019. Cortical mitochondria regulate insulin secretion by local Ca2+ buffering in rodent beta cells. Journal of Cell Science 132(9): jcs228544, Doi: 10.1242/jcs.228544.

[46] Ackermann, A.M., Zhang, J., Heller, A., Briker, A., Kaestner, K.H., 2017. High-fidelity Glucagon-CreER mouse line generated by CRISPR-Cas9 assisted gene targeting. Molecular Metabolism 6(3): 236–44, Doi: 10.1016/j.molmet.2017.01.003.

[47] Merrins, M.J., Poudel, C., McKenna, J.P., Ha, J., Sherman, A., Bertram, R., et al., 2016. Phase Analysis of Metabolic Oscillations and Membrane Potential in Pancreatic Islet β-Cells. Biophysical Journal 110(3): 691–9, Doi: 10.1016/j.bpj.2015.12.029.